Article

Emulsion Doping of Ionophores and Ion-Exchangers into Ion-Selective Electrode Membranes

SODA, Yoshiki, *et al*.

Abstract

Ion-selective electrodes (ISEs) are widely used analytical devices to selectively measure ionic species. Despite significant advances in recent years, ion-selective membranes are still mostly prepared in the same manner, by preloading the selective components into a solvent that is subsequently cast into a membrane or film. This paper describes an alternative method to prepare ISE membranes by mass transfer of the sensing components from an emulsion phase. Specifically, blank (undoped) plasticized poly(vinyl chloride) (PVC) membranes mounted into an electrode body are immersed into an aqueous solution containing analyte ions and an appropriate emulsion of the desired sensing components to allow their transfer into the membrane. The concept is demonstrated with conventional membrane electrodes containing an inner solution as well as all-solidstate electrodes. It is shown to be universally useful for the realization of ISEs for K+, Na+, Ca2+, and NO3−.

Reference

SODA, Yoshiki, *et al*. Emulsion Doping of Ionophores and Ion-Exchangers into Ion-Selective Electrode Membranes. *Analytical Chemistry*, 2020, vol. 92, no. 21, p. 14319-14324

DOI : 10.1021/acs.analchem.0c02920
PMID : 33084307

analytical chemistry

pubs.acs.org/ac

Technical Note

Emulsion Doping of Ionophores and Ion-Exchangers into Ion-Selective Electrode Membranes

Yoshiki Soda, Wenyue Gao, Jérôme Bosset, and Eric Bakker*

Cite This: *Anal. Chem.* 2020, 92, 14319−14324

Read Online

ACCESS | Metrics & More | Article Recommendations | Supporting Information

ABSTRACT: Ion-selective electrodes (ISEs) are widely used analytical devices to selectively measure ionic species. Despite significant advances in recent years, ion-selective membranes are still mostly prepared in the same manner, by preloading the selective components into a solvent that is subsequently cast into a membrane or film. This paper describes an alternative method to prepare ISE membranes by mass transfer of the sensing components from an emulsion phase. Specifically, blank (undoped) plasticized poly(vinyl chloride) (PVC) membranes mounted into an electrode body are immersed into an aqueous solution containing analyte ions and an appropriate emulsion of the desired sensing components to allow their transfer into the membrane. The concept is demonstrated with conventional membrane electrodes containing an inner solution as well as all-solid-state electrodes. It is shown to be universally useful for the realization of ISEs for K^+, Na^+, Ca^{2+}, and NO_3^-.

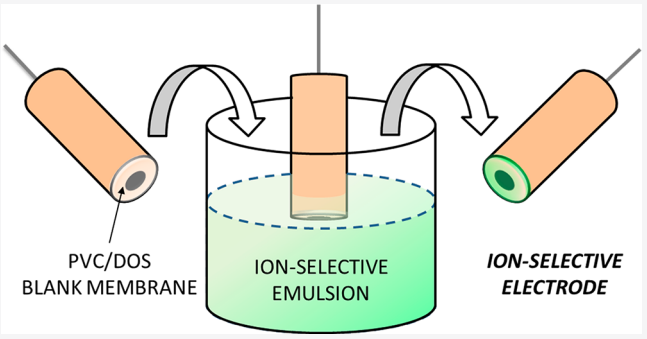

Ion-selective electrodes (ISEs)[1] are commonly used sensors to detect ionic species. Many efforts have been made to enhance the sensitivity and selectivity to analyte ions[2−6] and expand the sensor capability from inorganic ions[7] to biologically relevant polyions,[8,9] making these tools important in clinical and environmental research.[10,11] More recently, solid-contact ISEs with solid or polymeric ion to electron transducing materials[12,13] have started to replace the aqueous inner solution in liquid-membrane ISEs. This has expanded the applicability of ISEs and, for example, paved the way for in vivo assays with ultramicroelectrodes.[14]

Despite this progress, researchers have essentially relied on a single method to prepare ion-selective membranes. To endow the membrane with the desired selectivity and permselective behavior, the sensing components (i.e., ionophore and lipophilic ion-exchanger) are dissolved together with the membrane matrix components in an organic solvent. After its evaporation, the resulting membrane is conditioned, typically overnight, to replace the mobile ions with the ion to be measured. If the membrane exhibits comparably low mobility, proper conditioning may remain incomplete, which limits the available choices for the membrane matrix. A subsequent treatment of the membrane should not negatively affect the membrane components. Consequently, chemical functionalization may only be possible under very mild conditions, such as click chemistry,[15,16] because thermal[17,18] or UV treatments[19] can result in degradation. It would therefore be desired to separate the membrane preparation and mounting steps from the addition of the selective chemical components.

This technical note presents a new method to prepare ISE membranes. The underlying membrane preparation step is generic and only involves the matrix components. Subsequently, the selective components responsible for sensing are doped from aqueous solution, which is controlled by mass transport. Recent work has found that lipophilic ion-exchanger encapsulated in an aqueous microemulsion phase was able to contaminate an ion-selective membrane.[20] In this manner, the permselectivity of the membrane could be reversed, rendering a cation responsive membrane (initially containing a cation-exchanger) anion responsive by exposure to an emulsified anion-exchanger. We postulate here that the same mass transfer principle may be applied to most ionophores and that the general approach could be used to render blank membranes ion-selective. Several groups studied the mass transport of sensing components between two membranes[21,22] but not between an emulsified phase and the membrane.

This study first demonstrates the doping of ion-selective membranes from emulsion by a fluorescent dye, using confocal microscopy. The simultaneous doping of ionophore and cation-exchanger is established with valinomycin as a model system, using aqueous and solid inner contact electrodes. The

Received: July 9, 2020
Accepted: October 7, 2020
Published: October 21, 2020

https://dx.doi.org/10.1021/acs.analchem.0c02920
Anal. Chem. 2020, 92, 14319−14324

approach is then made more universal by optimization of the experimental conditions, realizing electrodes selective for K^+, Na^+, Ca^{2+}, NO_3^-. A further conditioning step is found to be unnecessary because selective ion-exchange of the initial counterion of the ion-exchanger already occurred in the ionophore-doped emulsion phase.[23]

EXPERIMENTAL SECTION

Chemicals and Tools. Electrode bodies for liquid-membrane electrodes were purchased from Oesch Sensor Technology (Sargans, Switzerland). Glassy carbon electrodes were sourced from Metrohm (Herisau, Switzerland). Poly(vinyl chloride) (PVC), dioctyl sebacate (DOS), sodium (or potassium) tetrakis[3,5-bis(trifluoromethyl)phenyl]borate (NaTFPB or KTFPB), valinomycin, calcium ionophore II (Ca-II), sodium ionophore X (Na-X), tridodecylmethylammonium nitrate ($TDMANO_3$), and tetrahydrofuran (THF) of Selectophore grade were all purchased from Sigma-Aldrich (St. Louis, MO). Confocal Zeiss LSM800 with 20× 0.8NA air objective (ZEISS, Oberkochen, Germany) was used to observe the mass transfer of dye into a polymeric membrane. Ag/AgCl/3 M KCl/1 M LiOAc reference electrode (Metrohm Autolab Utrecht, The Netherlands) connected to a high-impedance input 16-channel EMF monitor (Lawson Laboratories, Inc., Philadelphia, PA) was used for all potentiometry experiments.

Preparation of Membrane Electrodes with Inner Solution (K^+-Selective Electrodes Only). 60 mg of PVC and 120 mg of DOS were dissolved in 2 mL of THF followed by pouring this mixture into a glass ring (22 mm diameter) fixed on a glass plate. THF was allowed to evaporate overnight at room temperature, forming a plasticized PVC mother membrane that was then cut into circular pieces of 8 mm diameter that were mechanically mounted into Ostec electrode bodies. The electrode bodies were filled with 10 mM KCl solution as an inner solution.

Preparation of All-Solid-State Electrodes. Glassy carbon electrodes were carefully polished and fixed on styrofoam with the carbon face up. Ten μL of 4 mg mL^{-1} poly(3-octylthiophene) (POT) or multiwalled carbon nanotubes (MWCNTs) in chloroform was dropped on the glassy carbon surface. After drying for 30 min at room temperature, 50 μL of THF solution containing PVC and DOS (34 and 66 mg mL^{-1}) was dropped on the electrodes. The membrane coating was repeated 5 times at 20 min intervals.

Preparation of Polymeric and Matrix-Free Emulsion and Implementation of Mass Transfer. For the mass transfer of valinomycin and KTFPB from polymeric emulsion, 29 mmol kg^{-1} of valinomycin, 10 mmol kg^{-1} of KTFPB, 16 mg of PVC, and 32 mg of DOS were dissolved in 2 mL of THF. The mixture was injected into 35 mL of 10 mM KCl aqueous solution with 0.1 wt % Pluronic F-127 as a particle stabilizer to prevent particle aggregation. THF was allowed to evaporate from the aqueous solution by blowing compressed air for 1 h. On the other hand, electrode bodies (either liquid-membrane or all-solid-state ones) were soaked into 35 mL of 10 mM KCl aqueous solution and kept until the potentiometric signal stabilized. While continuously recording the cell potential, all of the 35 mL of polymeric emulsion solution was injected into the solution phase with stirring approximately at 300 rpm. For the mass transfer of Na-X and NaTFPB, the experimental procedure was chosen, but valinomycin and KTFPB were replaced with Na-X and NaTFPB at the same molar concentration (see Figure S1 for the experimental setup).

To implement mass transfer in the matrix-free emulsion system, 1.4 mmol of ionophore and 0.5 mmol of ion-exchanger were dissolved in 200 μL of DMF. The combination of ionophore/ion-exchanger was valinomycin/KTFPB for the fabrication of potassium-selective electrodes, Na-X/NaTFPB for detecting sodium, and Ca-II/KTFPB for calcium. For nitrate detection, just 1.4 mmol of $TDMANO_3$ was dissolved. The DMF solution was injected into 20 mL of aqueous solution containing 10 mM chloride salt of the analyte cation (KCl, NaCl, and $CaCl_2$) or $NaNO_3$ to reflect the analyte ion to be measured. Electrode bodies were in advance immersed in 50 mL of the corresponding aqueous salt solution containing 10 mM analyte ion salt, then the 20 mL matrix-free emulsion was injected into the electrode compartment while stirring at ~300 rpm.

Potentiometric Measurements. The procedure of potentiometry experiments was the same for any ionic species. 1 M and 10^{-3} M of each salt were prepared as stock solutions. The indicator electrodes and a double-junction Ag/AgCl/3 M KCl/1 M LiOAc reference electrode were connected to a high impedance input 16-channel EMF monitor (Lawson Laboratories, Inc., Malvern, PA) and were soaked into 70 mL of deionized water in a 100 mL beaker. After the potentiometric signal stabilized, 7 μL of 10^{-3} M solution was pipetted into the beaker, and subsequently, twice of each 35 and 350 μL of 10^{-3} M and 3.5, 35, 350, and 3500 μL of 1 M salt solution were added in this sequence every time the potentiometric response was found to be stable. Potential signal was analyzed as a function of the activity of the target ions. The theoretical Nernstian or half-Nernstian slopes were used to calculate selectivity coefficient for each ISEs.

Visualization of Mass Transport. 30 mmol kg^{-1} of Thioflavin T chloride, 30 mmol kg^{-1} of NaTFPB, 16 mg of PVC, and 32 mg of DOS, or 30 mmol kg^{-1} of Chromoionophore I (CH1), 16 mg of PVC, and 32 mg of DOS were dissolved in 2 mL of THF while the emulsion was prepared as above. A plasticized membrane as above was placed on the wall of a 100 mL beaker to which 35 mL of the emulsion was added. The membranes were kept in the beaker for 1 and 5 h, then kept frozen until microscopic observation. Confocal Zeiss LSM800 with 20× 0.8NA air objective was used for confocal microscopic observation with 405 nm excitation light. The target membrane was placed horizontally on a slide glass. The beginning and end of the fluorescent signal were investigated and defined as the top and bottom of the membrane, and in turn, images from the outer to the inner side of the membrane were taken at depth increments of 2 μm.

RESULTS AND DISCUSSION

Mass transfer of ionophore and ion-exchanger from polymeric emulsions composed of poly(vinyl chloride) (PVC) plasticized with dioctyl sebacate (DOS) at a ratio of 1:2 containing valinomycin and KTFPB was established. $TFPB^-$ having potassium as a counterion was chosen in order to exclude the ion exchange process and observe only ionophore/ion-exchanger transfer as a model experiment. A schematic illustration of the experimental setup is shown in Figure S1. The visualization of mass transport by confocal microscopy, potential changes over the course of mass transfer, and the resulting potentiometric response to K^+ and Na^+ to demonstrate selectivity are shown in Figure 1.

https://dx.doi.org/10.1021/acs.analchem.0c02920
Anal. Chem. 2020, 92, 14319−14324

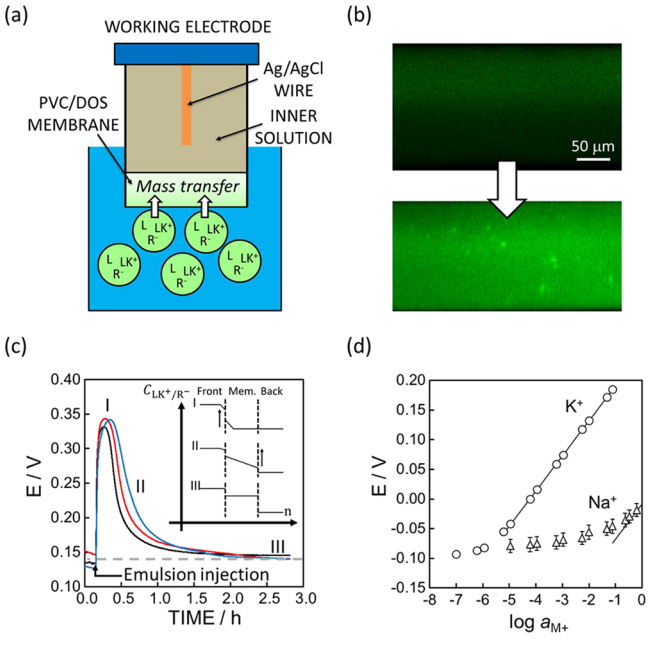

Figure 1. (a) Schematic illustration of ionophore/ion exchanger mass transport from an emulsion phase to a blank membrane, (b) Confocal microscopy images of membranes prepared after doping for a period of either 1 h (top) or 5 h (bottom) with Thioflavin T (ThT)/TFPB$^-$. The brightness and contrast of the top image (1 h mass transport) was adjusted to better visualize the signal gradients brightness: +40%, contrast: +20%. Observed membrane thickness ~160 μm. (c) Potential−time change over the course of mass transfer of valinomycin/KTFPB (black line). (d) Potentiometric measurement for potassium as primary and sodium as model interfering ionic species (log $K^{pot}_{K+,Na+} = -4.5$). Solid lines are with theoretical Nernstian slope.

To visually confirm the concept, Thioflavin T (ThT), a positively charged dye (which should be difficult to transfer owing to its high hydrophilicity), with NaTFPB as anion additive, was transferred from PVC emulsion to the bulk membrane and the fluorescence signal was observed by confocal microscopy. The images in Figure 1b shows the transient extraction (0.5 h) and complete penetration (5 h) of the ThT$^+$/TFPB$^-$ pair into the membrane. This indicates the feasibility of mass transfer of lipophilic molecules from the emulsion phase to the membrane. A much more lipophilic fluorescent ionophore, chromoionophore I, was also found to penetrate throughout the membrane as shown in Figure S8. These results suggest that valinomycin and ion-exchanger are also expected to be transported into the bulk of the membrane. This should be driven by a concentration gradient upon contact of the emulsified ingredients with the membrane as illustrated in Figure 1a. If so, the membrane side of the phase boundary should start to be loaded with valinomycin/KTFPB. Owing to the strong binding interaction of valinomycin to K$^+$, the concentration of free K$^+$ should drastically decrease. A positive potential jump accompanies this process, which was indeed observed experimentally (see stage I in Figure 1c). Once valinomycin reaches the backside of the membrane surface upon prolonged contact, the reverse process should take place at that side. Indeed, the potential is found to decrease back to near the initial potential (stage II of Figure 1c). This is found to be a continuous process until the concentrations within the membrane become symmetric (stage III of Figure 1c).

The reduction in potential drift (see Figure 1c) serves as an indicator for the attainment of doping equilibrium. For this experiment it takes ~4 h for adequate ionophore/ion exchanger transfer and to approach an equilibration throughout the membrane. Note that the initial potential before the onset of ionophore transfer is theoretically 136 mV (10 mM and 3 M of inner solutions for the working and reference electrodes, respectively), which is indicated as a broken gray line in Figure 1c.

The emulsified PVC particles used to dope the membrane were stabilized by the surfactant F-127 to prevent PVC particles from aggregating. F-127 is not required as an emulsion matrix but as a particle stabilizer. The transfer of components from the emulsified particles and the membrane phase may depend on their ability to overcome the hydrophilic boundary formed by F-127. It is therefore not immediately obvious that this type of doping approach should be successful. Indeed, as shown below, different ionophores do not exhibit the same doping behavior.

Figure 1d shows the potentiometric response to the primary ion K$^+$ and a selected interfering ion Na$^+$ after an emulsion doping time of 4 h. The expected Nernstian response to K$^+$ is observed (59.1 mV) while the response to Na$^+$ is apparently half Nernstian (29.9 mV) at high concentration (see the caption of Table 1) in agreement with earlier studies that explain the potentiometric response during the course of

Table 1. List of the Ionophore/Ion-Exchanger Component Pairs Used to Prepare Solid-State Electrodes by Mass Transfer, PVC/DOS Ratio of Membrane Mounted on Electrodes, Emulsion Matrixes for Each Experiment, and the Physical Properties of Prepared Electrodes

transported components	PVC−DOS (solid ISE membrane)	emulsion matrix	primary ion/slope (mV)	interfering ion/slope (mV)	log $K^{pot}_{i,j}$
valinomycin/KTFPB	1:2	PVC/DOS (1:2)	K$^+$/57.3	Na$^+$/32.3[b]	−4.4 ± 0.3
valinomycin/KTFPB	1:2	DMF	K$^+$/54.8	Na$^+$/28.8[b]	−4.7 ± 0.2
valinomycin/KTFPB	3:1	PVC/DOS (3:1)	K$^+$/52.3	Na$^+$/26.0[b]	−4.2 ± 0.1
Na-X/NaTFPB	1:2	PVC/DOS (1:2)	Na$^+$/34.5	K$^+$/N/A	N/A[a]
Na-X/NaTFPB	1:2	Pluronic F-127/DOS (1:2)	Na$^+$/30.5	K$^+$/N/A	N/A[a]
Na-X/NaTFPB	1:2	DMF	Na$^+$/59.0	K$^+$/53.9	−2.5 ± 0.1
CaII/KTFPB	1:2	DMF	Ca^{2+}/29.6	Mg^{2+}/17.7[c]	−5.0 ± 0.2
TDMACNO$_3$	1:2	DMF	NO$_3^-$/−55.6	Cl$^-$/−55.6	−1.9 ± 0.2

[a]Mass transfer was not implementable with the indicated experimental conditions. See the Results and Discussion above for details. [b]The slope is obtained from the linear curve fit with Na$^+$ concentrations higher than 10^{-1} M (3 highest points). [c]The slope is obtained from the linear curve fit with the Mg^{2+} concentrations higher than $10^{-3.1}$ M (5 highest points).

https://dx.doi.org/10.1021/acs.analchem.0c02920
Anal. Chem. 2020, 92, 14319−14324

incomplete ion exchange between primary and interfering ions.[24−26] The data give an apparent logarithmic selectivity coefficient of log $K^{pot}_{K+,Na+}$ = −4.5, in agreement with the literature values for valinomycin-based ion-selective electrodes.[7]

This mass transfer phenomenon was also applied to prepare solid-state electrodes composed of glassy carbon electrodes containing a poly(3-octylthiophene) (POT) transduction layer covered with a PVC−DOS (1:2) membrane (see Figure 2a).

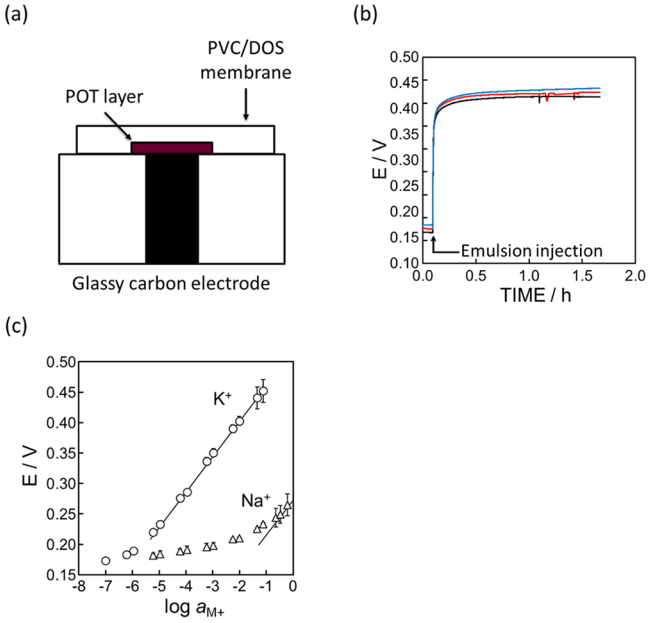

Figure 2. (a) Schematic illustration of the solid-state electrode. (b) Potential-time trace upon addition of plasticized PVC-based emulsion containing valinomycin and KTFPB. (c) Resulting potentiometric response to potassium and sodium ions after doping (log $K^{pot}_{K+,Na+}$ = −4.4). Solid lines are Nernstian (see Table 1 for the experimental slopes).

From the observed potential drift during the doping process (Figure 2b), mass transfer was complete within ∼1 h. This is a considerably shorter time than with the liquid-membrane electrodes shown in Figure 1. Potentiometric responses to primary and interfering ionic species were again assessed after potential stabilization, see Figure 2c. The selectivity was comparable to that of the corresponding valinomycin-based liquid-membrane ISEs.

The considerably shorter conditioning period observed with solid-state electrodes does not represent a fully equilibrated state. Indeed, when the solid-state electrodes in contact with the emulsified sensing components are measured for a longer time (see Figure S2), a partial reversal of the potential by ∼100 mV after about 3 h is observed. This is likely due to a potential change at the buried ion-to-electron transduction layer caused by the diffusing sensing components, but this was not studied in further detail. This intermediate state is very stable in the time scale of the potentiometric experiment (see Figure 2b), and the electrodes are therefore usable with very short doping/conditioning times.

If one seeks a more rapid full equilibration with the emulsion phase, it could be achieved by preparing thinner membranes. Alternatively, the potential reversal process may be suppressed with less diffusive membrane materials. Indeed, a membrane containing a lower plasticizer content (PVC−DOS = 3:1) shows a stable potentiometric signal over the course of a 16 h doping period with a polymeric emulsion of the same PVC−DOS ratio, see Figure S3a. This less diffusive membrane adequately maintains the expected potentiometric response and selectivity (see Figure S3b). However, it is noted that the initial potential jump is smaller for this formulation. While one may want to ascribe this to a smaller complex formation constant, it could equally be explained by a less efficient doping process. Indeed, a higher plasticizer content has been reported to increase the partition coefficient.[27]

The mass transfer rate from PVC−DOS-based emulsions appears to strongly depend on the type of ionophore. With the sodium ionophore X (Na-X), the same polymeric emulsion system did not appear to induce the desired mass transport. Figure S4a,c show the potentiometric time trace for the attempted doping of Na-X/NaTFPB from either PVC−DOS (1:2) or Pluronic F-127/DOS (1:2) emulsions to solid-state electrodes having a PVC−DOS (1:2) membrane in analogy to that in Figure 2a, respectively. The very modest potential jump observed upon introducing the emulsion suggests insufficient doping, which is confirmed by the sub-Nernstian sodium response slopes in Figure S4b,d. Perhaps the hydrophilic barrier from the F-127 coating inhibits efficient mass transfer of some hydrophobic species into the membrane.

Recent work suggested that a matrix-free emulsion may be formed in the presence of the water miscible organic solvent tetrahydrofran (THF), without any addition of plasticizer or PVC.[23] This concept was explored here for the transfer of Na-X/NaTFPB but with the solvent *N*,*N*-dimethylformamide (DMF) instead of THF because of its higher boiling point. The procedure was otherwise analogous to that with the polymer-based emulsions described above, see the Experimental Section. As shown in Figure S5a, the amplitude of the initial potential jump upon injection of a Na-X/NaTFPB emulsion was about 120 mV. This change is significantly larger than with the polymeric emulsion systems shown in Figure S4a,c, but it seems more modest than for valinomycin. Nonetheless, Figure 3a demonstrates a Nernstian response slope to sodium and a selectivity over potassium that is comparable with literature values based on this ionophore.[7]

This DMF-based matrix-free system was also confirmed to be applicable to valinomycin as shown in Figure S6a,b. Calcium selectivity was achieved with the same matrix-free system but with calcium ionophore II (Ca-II) and KTFPB. This experiment differs from that for valinomycin and Na-X because it involves a counterion of $TFPB^-$ that is not the analyte ion. The signal showed an abrupt potential jump (see Figure S5b), and the potentiometric time traces to calcium and the corresponding selectivity over magnesium are comparable with the literature values (see Figure 3b).[28] With traditional protocols, one typically requires to condition the prepared membrane in Ca^{2+} solution, but this is not necessary here as the emulsion was prepared in a calcium electrolyte. Spontaneous ion-exchange is expected to occur for the emulsion, as reported before,[23] resulting in a preconditioning of the emulsion phase with calcium. A single procedure to prepare the ion-selective membrane appears to be sufficient that combines doping and conditioning into a single step.

Anion-selective electrodes were prepared with the same mass transfer principle. As one most widely studied analyte, nitrate was chosen as a target ionic species based on the anion-exchanger tridodecylmethylammonium nitrate ($TDMANO_3$).

https://dx.doi.org/10.1021/acs.analchem.0c02920
Anal. Chem. 2020, 92, 14319−14324

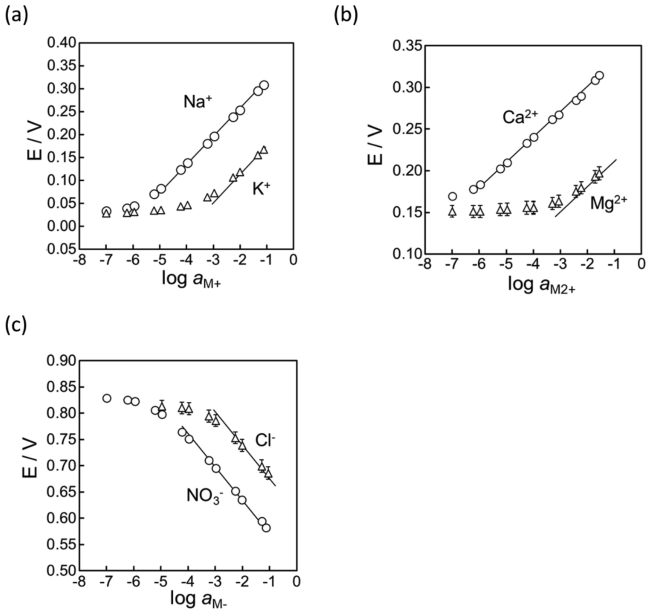

Figure 3. Potentiometric responses to the primary and an important interfering ion after preparating solid-state electrodes by doping with (a) Na-X/NaTFPB, (b) Ca-II/KTFPB, and (c) $TDMANO_3$ (giving log $K^{pot}_{K+,Na+} = -2.5$, log $K^{pot}_{Ca2+,Mg2+} = -5.0$, log$K^{pot}_{NO3-,Mg2+} = -1.9$). Solid lines are Nernstian, see Table 1 for experimental slopes.

On the basis of earlier work,[29] multiwalled carbon nanotubes (MWCNTs) were used as transduction layer for better potentiometric stability. The potential jump seen in Figure S5c is explained by the increase of nitrate concentration in the membrane because ion-paring of $TDMA^+$ and nitrate is considered to be limited. The potentiometric responses to nitrate and chloride suggest an appropriate Nernstian response to nitrate and a selectivity over chloride that compares well to earlier work (see Figure 3c and Table 1).[30]

These electrodes did not show a second transition at longer doping times (see Figure S7), which is attractive for practical use. As above, electrodes with thinner membranes should equilibrate more quickly or, alternatively, a less diffusive membrane may be used to retain a semisteady state with acceptable potential stability for a longer time (see Figure S3).

Exposure of a valinomycin-based membrane to a solution containing blank (ionophore-free) F127−DOS (1:2) were also evaluated and gave a negligible potential change with time, see Figure S9. This suggests that the ionophore is not readily back extracted in this manner.

CONCLUSION

A new method is developed here to prepare ion-selective electrode membranes where the active sensing components (ionophores and ion-exchangers) are transferred from an emulsified phase to the polymeric membrane of interest. By using matrix-free emulsion systems the approach is found to be rather universal and applicable for a wide range of selective components. This is in contrast to polymeric emulsions that did not work for all systems. Still, a polymeric emulsion system remains an attractive choice owing to its compatibility with the electrode membrane. In the second approach, the added organic solvent will likely partition into the membrane and may result in swelling. This should increase mass transport, which is welcome but could also give rise to memory effects that call for the need to remove this solvent after doping. Eventually, the approach used here could form the basis for a repetitive extraction/redoping of membrane components, which is currently being explored in our laboratory.

ASSOCIATED CONTENT

Supporting Information

The Supporting Information is available free of charge at https://pubs.acs.org/doi/10.1021/acs.analchem.0c02920.

14-h potential tracking of all-solid-state electrodes fabricated with plasticized PVC (PVC−DOS = 1:2) in matrix-free system; 16-h potential tracking of all-solid-state electrodes fabricated with plasticized PVC (PVC−DOS = 3:1) in matrix-free system and their potentiometric experiment with K^+ and Na^+; potential tracking and the corresponding potentiometry experiments for all-solid-state electrodes put in the PVC/DOS or Pluronic F-127 emulsion system containing Na-X and NaTFPB; potential tracking and the potentiometry experiment of all-solid-state electrodes in the DMF-based matrix-free emulsion system; and microscopic image of chromoionophore I diffusing into the membrane bulk (PDF)

AUTHOR INFORMATION

Corresponding Author

Eric Bakker − *Department of Inorganic and Analytical Chemistry, University of Geneva, CH-1211 Geneva, Switzerland;* orcid.org/0000-0001-8970-4343; Email: Eric.Bakker@unige.ch

Authors

Yoshiki Soda − *Department of Inorganic and Analytical Chemistry, University of Geneva, CH-1211 Geneva, Switzerland*

Wenyue Gao − *Department of Inorganic and Analytical Chemistry, University of Geneva, CH-1211 Geneva, Switzerland*

Jérôme Bosset − *BioImaging Center, Department of Biochemistry, University of Geneva, CH-1211 Geneva, Switzerland*

Complete contact information is available at: https://pubs.acs.org/10.1021/acs.analchem.0c02920

Author Contributions

Conceptualization, Y.S. and E.B.; methodology, Y.S. and E.B.; experiment, Y.S.; technical advice for anion-selective electrodes, W.G.; confocal microscopic images were taken by J.B. All authors have given approval to the final version of the manuscript.

Notes

The authors declare no competing financial interest.

ACKNOWLEDGMENTS

This work was supported by the Swiss National Science Foundation.

REFERENCES

(1) Bakker, E.; Bühlmann, P.; Pretsch, E. *Chem. Rev.* **1997**, *97* (8), 3083−3132.

(2) Amemiya, S.; Bühlmann, P.; Umezawa, Y. *Anal. Chem.* **1998**, *70* (3), 445−454.

(3) Bakker, E.; Bühlmann, P.; Pretsch, E. *Talanta* **2004**, *63* (1), 3−20.

(4) Zdrachek, E.; Bakker, E. *Anal. Chem.* **2020**, *92* (4), 2926−2930.

(5) Vigassy, T.; Morf, W. E.; Badertscher, M.; Ceresa, A.; de Rooij, N. F.; Pretsch, E. *Sens. Actuators, B* **2001**, *76*, 477−482.
(6) Eugster, R.; Gehrig, P. M.; Morf, W. E.; Spichiger, U. E.; Simon, W. *Anal. Chem.* **1991**, *63* (20), 2285−2289.
(7) Bühlmann, P.; Pretsch, E.; Bakker, E. *Chem. Rev.* **1998**, *98* (4), 1593−1688.
(8) Ma, S. C.; Yang, V. C.; Meyerhoff, M. E. *Anal. Chem.* **1992**, *64* (6), 694−697.
(9) Mathison, S.; Bakker, E. *Anal. Chem.* **1999**, *71* (20), 4614−4621.
(10) Lewenstam, A.; Maj-Zurawska, M.; Hulanicki, A. *Electroanalysis* **1991**, *3* (8), 727−734.
(11) Dimeski, G.; Badrick, T.; John, A. S. *Clin. Chim. Acta* **2010**, *411* (5), 309−317.
(12) Michalska, A. *Electroanalysis* **2012**, *24* (6), 1253−1265.
(13) Bobacka, J.; Ivaska, A.; Lewenstam, A. *Chem. Rev.* **2008**, *108* (2), 329−351.
(14) Lindner, E.; Buck, R. P. *Anal. Chem.* **2000**, *72* (9), 336 A−345 A.
(15) Pawlak, M.; Mistlberger, G.; Bakker, E. *J. Mater. Chem.* **2012**, *22* (25), 12796−12801.
(16) Pawlak, M.; Grygolowicz-Pawlak, E.; Crespo, G. A.; Mistlberger, G.; Bakker, E. *Electroanalysis* **2013**, *25* (8), 1840−1846.
(17) Mir, M.; Lugo, R.; Tahirbegi, I. B.; Samitier, J. *Sensors* **2014**, *14* (7), 11844−11854.
(18) Yang, C.-C.; Wu, G. M. *Mater. Chem. Phys.* **2009**, *114* (2), 948−955.
(19) Abramova, N.; Bratov, A. *Sensors* **2009**, *9* (9), 7097−7110.
(20) Apichai, S.; Wang, L.; Pankratova, N.; Grudpan, K.; Bakker, E. *Electroanalysis* **2018**, *30* (10), 2462−2466.
(21) Akieh-Pirkanniemi, M.; Lisak, G.; Arroyo, J.; Bobacka, J.; Ivaska, A. *J. Membr. Sci.* **2016**, *511*, 76−83.
(22) Mi, Y.; Bakker, E. *Anal. Chem.* **1999**, *71* (23), 5279−5287.
(23) Wang, L.; Sadler, S.; Cao, T.; Xie, X.; Von Filseck, J. M.; Bakker, E. *Anal. Chem.* **2019**, *91* (14), 8973−8978.
(24) Bakker, E.; Pretsch, E. *TrAC, Trends Anal. Chem.* **2001**, *20* (1), 11−19.
(25) Ceresa, A.; Radu, A.; Peper, S.; Bakker, E.; Pretsch, E. *Anal. Chem.* **2002**, *74* (16), 4027−4036.
(26) Bakker, E.; Bühlmann, P.; Pretsch, E. *Talanta* **2004**, *63* (1), 3−20.
(27) Oesch, U.; Simon, W. *Anal. Chem.* **1980**, *52* (4), 692−700.
(28) Bedlechowicz-Śliwakowska, I.; Lingenfelter, P.; Sokalski, T.; Lewenstam, A.; Maj-Żurawska, M. *Anal. Bioanal. Chem.* **2006**, *385* (8), 1477−1482.
(29) Yuan, D.; Anthis, A. H. C.; Ghahraman Afshar, M.; Pankratova, N.; Cuartero, M.; Crespo, G. A.; Bakker, E. *Anal. Chem.* **2015**, *87* (17), 8640−8645.
(30) Zhai, J.; Xie, X.; Bakker, E. *Anal. Chem.* **2015**, *87* (16), 8347−8352.

https://dx.doi.org/10.1021/acs.analchem.0c02920
Anal. Chem. 2020, 92, 14319−14324